

# Including a Battery State of Health model in the HEV component sizing and optimal control problem <sup>★</sup>

Lars Johannesson <sup>\*</sup> Nikolce Murgovski <sup>\*\*</sup> Soren Ebbesen <sup>\*\*\*</sup>  
Bo Egardt <sup>\*\*</sup> Esteban Gelso <sup>\*\*\*\*</sup> Jonas Hellgren <sup>\*\*\*\*</sup>

<sup>\*</sup> *Signals and Systems/Electromobility, Chalmers University of Technology/Viktoria Institute, Göteborg, 412 96/417 56 Sweden (e-mail: larsjo@chalmers.se/lars.johannesson@viktoria.se).*

<sup>\*\*</sup> *Signals and Systems, Chalmers University of Technology, Göteborg, 412 96 Sweden (e-mails: nikolce.murgovski@chalmers.se, bo.egardt@chalmers.se).*

<sup>\*\*\*</sup> *Dept. of Mechanical and Process Engineering, ETH Zurich, 8092 Zurich, Switzerland (e-mail: sebbesen@ethz.ch)*

<sup>\*\*\*\*</sup> *Group Trucks Technology, Volvo, Göteborg, 412 58 Sweden, (e-mail: esteban.gelso@volvo.com, jonas.hellgren@volvo.com)*

---

**Abstract:** This paper studies convex optimization and modelling for component sizing and optimal energy management control of hybrid electric vehicles. The novelty in the paper is the modeling steps required to include a battery wear model into the convex optimization problem. The convex modeling steps are described for the example of battery sizing and simultaneous optimal control of a series hybrid electric bus driving along a perfectly known bus line. Using the proposed convex optimization method and battery wear model, the city bus example is used to study a relevant question: is it better to choose one large battery that is sized to survive the entire lifespan of the bus, or is it beneficial with several smaller replaceable batteries which could be operated at higher c-rates?

*Keywords:* hybrid electric vehicle, convex optimization, batteries, optimal dimensioning and control, battery state of health.

---

## 1. INTRODUCTION

Investigations about the cost effectiveness of a future Hybrid Electric Vehicle (HEV) require detailed knowledge on several system levels as well as price scenarios for components, fuel, electricity etc. Considering the many ways of constructing a hybrid electric powertrain and the high degree of freedom in sizing the individual powertrain components to emphasize different characteristics of the powertrain, there is a strong need for systematic approaches.

A complicating factor for early concept studies of HEVs and PHEVs is that the energy efficiency of the powertrain depends on how well adapted the energy management strategy, controlling the energy flows in and out of the electric energy buffer, is to the specific vehicle concept and its intended driving. Many researchers have addressed this optimal control problem using Dynamic Programming (DP), see for instance Zoelch and Schroeder (1998), and Sundström et al. (2010). The main advantage with DP is the capability to use nonlinear, non-convex models of the components consisting of continuous and integer (mixed-integer) optimization variables. However, a serious limita-

tion of DP is that the computation time increases exponentially with the number of state variables. As a consequence, the powertrain model is typically limited to only one or possibly two continuous state variables. Moreover, since DP operates by recursively solving a smaller subproblem for each time step, the second limitation of DP is that it is not possible to directly include the component sizing into the optimization.

In more recent studies Murgovski et al. (2012b), and Murgovski et al. (2012a) another approach has been proposed that uses convex optimization to simultaneously size the battery in a PHEV while optimally controlling the energy flow.

This paper is an extension of Murgovski et al. (2012a), showing the necessary modeling steps to include the battery wear model proposed in Ebbesen et al. (2012) in the optimal component sizing and energy management problem. In Ebbesen et al. (2012) the battery wear is related to the energy throughput and c-rate.

An example is given for a HEV city bus of series topology. Using the proposed optimization method and battery wear model the example answers a relevant question: is it better to choose one large battery that is sized to survive the entire lifespan of the vehicle, or several smaller replaceable batteries which could be operated at higher c-rates?

---

<sup>★</sup> This research was funded by the Chalmers Energy Initiative and the Swedish Energy Agency in the FFI-project Integrated Vehicle Design and Control.

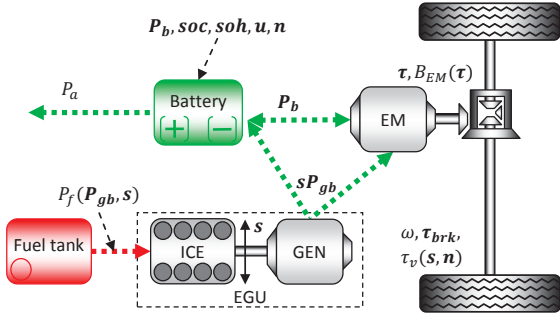


Fig. 1. Series PHEV powertrain model.

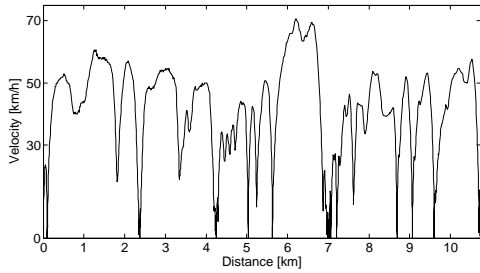


Fig. 2. Bus line model described by demanded velocity. For simplicity the road grade is zero at all times in the studied example.

The paper is outlined as follows: modeling details are given in Section 2 and 3, the optimization problem is then formulated in Section 4 and remodeled as convex in Section 5, the example of the optimal battery replacement strategy is given in Section 6, the paper ends with conclusion and discussion in Section 7.

## 2. BUS LINE AND POWERTRAIN MODEL

The studied HEV bus includes a powertrain in a series topology with no mechanical connection between the engine and the wheels, as in Fig. 1. Instead, the wheels are driven by an Electric Machine (EM) that receives energy from a battery and/or an Engine-Generator Unit (EGU).

The bus is driven on a bus line described by road gradient and demanded velocities which are known at each point of time (Fig. 2). The velocity and force demands from the bus line can be translated into an angular velocity  $\omega(t)$  and torque

$$\tau_v(\cdot) = \tau_b(t) + A_1(t)\mathbf{n}_b + A_2(t)s \quad (1)$$

on the shaft between the EM and the differential. The number of battery cells  $\mathbf{n}_b$  and the EGU size  $s$  are optimization variables (marked in bold), and  $(\cdot)$  is used as a compact notation to identify a function of optimization variables. The torque  $\tau_b(t)$  of the vehicle without the weight of the battery and EGU, and the time dependent terms  $A_j(t)$  are functions of the demanded acceleration and speed on the bus line and the known vehicle parameters, such as inertia, aerodynamic drag, rolling resistance, wheels radius, etc.

The EM delivers or regenerates the torque  $\tau(t)$ . The EM brake regeneration is either limited by its torque limit  $\tau_{min}(\omega(t))$ , or the buffer charging limit, after which friction

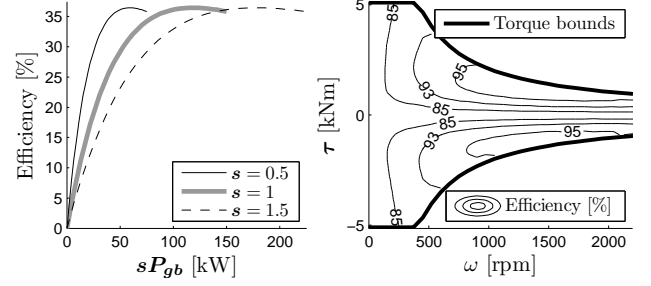


Fig. 3. Model of the EGU, left, and the EM, right. The figure illustrates the efficiency curves of the baseline EGU ( $s = 1$ ), the smallest allowed EGU ( $s = 0.5$ ), and the largest EGU ( $s = 1.5$ ).

brakes are used to handle the remaining braking torque  $\tau_{brk}(t)$ , i.e.

$$\tau(t) = \tau_v(\cdot) - \tau_{brk}(t). \quad (2)$$

The powertrain electric path is described by a power balance

$$\tau(t)\omega(t) + B_{EM}(\cdot) = \mathbf{P}_b(t) + s\mathbf{P}_{gb}(t) - P_a \quad (3)$$

that relates the EM electric power, left side of the equality, to the battery power  $\mathbf{P}_b(t)$ , EGU power  $s\mathbf{P}_{gb}(t)$  and power consumed by auxiliary devices  $P_a$ . The losses of the EM are modeled as a quadratic function on  $\tau(t)$

$$B_{EM}(\cdot) = b_0(\omega(t))\tau^2(t) + b_1(\omega(t))\tau(t) + b_2(\omega(t)) \quad (4)$$

with speed dependent coefficients:  $b_j(\omega(t)) \geq 0, j \in \{0, 2\}, \forall t \in [t_0, t_f]$ .

The generator power, EGU losses and mass are assumed to scale linearly with the generator power  $\mathbf{P}_{gb}(t)$ , losses  $B_{EGUb}(\cdot)$  and mass  $m_{EGUb}$  of a baseline EGU model with maximum power of  $P_{gbmax} = 150$  kW. Then, the fuel power  $P_f(\cdot)$  and mass  $m_{EGU}$  of the scaled EGU can be expressed as

$$P_f(\cdot) = s(\mathbf{P}_{gb}(t) + B_{EGUb}(\cdot)), \quad (5)$$

$$m_{EGU} = sm_{EGUb}, \quad (6)$$

$$s \in [0.5, 1.5]. \quad (7)$$

The losses of the baseline EGU are also modeled as quadratic

$$B_{EGUb}(\cdot) = a_0\mathbf{P}_{gb}^2(t) + a_1\mathbf{P}_{gb}(t) + a_2e(t) \quad (8)$$

with  $a_j \geq 0, j \in \{0, 2\}$ , where  $e(t)$  is a binary variable that is needed to allow zero fuel power, i.e. to remove the idling losses  $a_2$  when the engine is off. The efficiencies of the EM and EGU are illustrated in Fig. 3, while details on the validity of using quadratic losses for these components can be found in Murgovski et al. (2012b).

The engine on/off control is decided using heuristics that turn the engine on if the power of the vehicle without the weight of the energy buffer and EGU exceeds a threshold  $P_{on}^*$ , i.e.

$$e(t) = \begin{cases} 1, & \tau_b(t)\omega(t) > P_{on}^* \\ 0, & \text{otherwise.} \end{cases} \quad (9)$$

The optimal power threshold  $P_{on}^*$  is found by iteratively solving a convex optimization problem, described later in Section 4 and 5, for several values of  $P_{on}$  within the power range of the vehicle. In Murgovski et al. (2012b), this heuristics has been shown to give small error to the

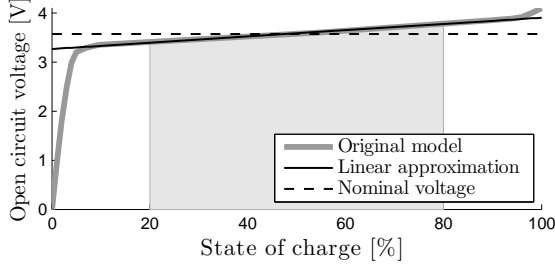


Fig. 4. Model of the battery open circuit voltage. The shaded region represents the allowed SOC range.

global optimum. The losses of the power electronics are for simplicity neglected.

### 3. BATTERY MODEL

The battery consists of identical cells equally divided in parallel strings, with the strings consisting of cells connected in series. The battery cells are modeled by a resistive circuit

$$\mathbf{P}_b(t) = (\mathbf{u}(t)i(\cdot) - R_c i^2(\cdot)) \mathbf{n}_b,$$

where  $\mathbf{P}_b(t)$  is the pack power,  $i(\cdot)$  is the cell current,  $\mathbf{n}_b$  is the total number of cells in the pack, and  $\mathbf{u}(t)$  is the open circuit voltage which is shown in Fig. 4 and is non-linear function SoC. Thus

$$i(\cdot) = \frac{1}{2R_c} \left( \mathbf{u}(t) - \sqrt{\mathbf{u}^2(t) - \frac{4R_c \mathbf{P}_b(t)}{\mathbf{n}_b}} \right), \quad (10a)$$

$$i(\cdot) \in [i_{min}, i_{max}], \quad (10b)$$

$$\mathbf{P}_b(t) \leq \frac{\mathbf{u}^2(t) \mathbf{n}_b}{4R_c}, \quad (10c)$$

where  $R_c$  is the inner resistance and  $i_{min}, i_{max}$  are the maximum and minimum cell current<sup>1</sup>. The battery State of Charge (SoC) dynamics and constraints are then written as

$$\dot{soc}(t) = -\frac{1}{Q} i(\cdot), \quad (11a)$$

$$soc(t) \in [soc_{min}, soc_{max}], \quad (11b)$$

$$soc(t_f) = soc(t_0). \quad (11c)$$

In the optimization  $\mathbf{n}_b$  has a real value that indicates the total pack capacity. It can be expected that rounding this variable to the nearest integer gives small error if results point to large number of cells. This will generally be the case if the cells are chosen small. Another way to use the optimization is to interpret the cell data as a relationship for specific energy and power for given battery technology. The assumption is then that the capacity of the actual cells to be used in the vehicle can be purposely built to fit the desired pack voltage and number of strings. With this assumption the optimal number of cells  $\mathbf{n}_b^*$  will point towards the optimal energy/charge capacity and battery pack power.

<sup>1</sup> The problem can alternatively be formulated to size the pack with fixed number of strings. The battery pack terminal voltage would then be constrained to be within the range specified by the inverter.

Table 1. Pre-exponential factor tabulated with respect to  $c$ -rate.

$c$	0.5	2	6	10
$B(c)$	31,630	21,681	12,934	15,512

#### 3.1 Battery wear model

The energy throughput-based battery state-of-health model from Ebbesen et al. (2012) is used in this paper. This model assumes that the battery can be cycled  $N$  times before the capacity has dropped by  $\Delta E_0 = 0.2E_0$  from the nominal energy capacity  $E_0$  (20% capacity drop is the common definition of end-of-life of the battery). In the model, the internal battery cell power  $P_i(\cdot)$  is intergrated and normalized by the total amount of energy that can be put through the battery cell before end-of-life, that is

$$soh(t) = 1 - \frac{1}{2N(|P_i(t)|)E_0(0)} \int_0^t |P_i(\tau)| d\tau. \quad (12)$$

Once the state-of-health  $soh(t) \in [0, 1]$  reaches zero, the battery has reached its end-of-life. The first order derivative of the state-of-health is

$$\dot{soh}(t) = -\frac{|P_i(t)|}{2N(|P_i(t)|)E_0}. \quad (13)$$

Note that a dependency of  $|P_i(t)|$  on  $N$  is included in order to differentiate the impact of the time-variant operating conditions on the state-of-health. Note that in the battery wear model the internal battery power is defined by the nominal open circuit voltage,  $\bar{U}$  (dashed line in Fig. 4), as  $P_i(\cdot) = \bar{U}i(\cdot)$ . The function  $N(|P_i(t)|)$  is defined by

$$N(|P_i(t)|) = \frac{\bar{U}A(|P_i(t)|/E_0)}{E_0}. \quad (14)$$

The variable  $A(c)$  is the total amp-hour throughput until the end-of-life when assuming that the battery cell is cycled with a constant  $c$ -rate and where  $c = P_i/E_0$ . The total amp-hour throughput until end-of-life is modeled as in I. Bloom et al. (2001)

$$A(c) = \left[ \frac{\Delta E_0}{B(c) \exp\left(\frac{-E_a(c)}{RT}\right)} \right]^{1/z}. \quad (15)$$

This relation is based on the Arrhenius equation in which  $B(c)$  is the pre-exponential factor, and  $E_a(c)$  is the activation energy, while  $R$  is the ideal gas constant,  $T$  is the lumped cell temperature, and  $z$  the power law factor.

The model was parameterized for the A123 Systems ANR26650M1 cell of 3.3V, 2.3Ah, using the data published in Wang et al. (2011). Equation (16) and Table 1 summarize the results of the parameterization.

$$\begin{aligned} E_a(c) &= (31700 - 370.3c) \text{ J/mol} \\ z &= 0.55 \\ R &= 8.31 \text{ J/mol}\cdot\text{K} \\ T &= 313 \text{ K (40}^\circ\text{C)} \end{aligned} \quad (16)$$

In Fig. 5,  $N(|P_i|)$  and  $\dot{soh}(|P_i|)$  are shown together with a piece-wise quadratic approximation of  $\dot{soh}(|P_i|)$ . Notice that the cell appears to withstand more cycles at an intermediate power level than at low power. This counterintuitive observation can be explained by the fact

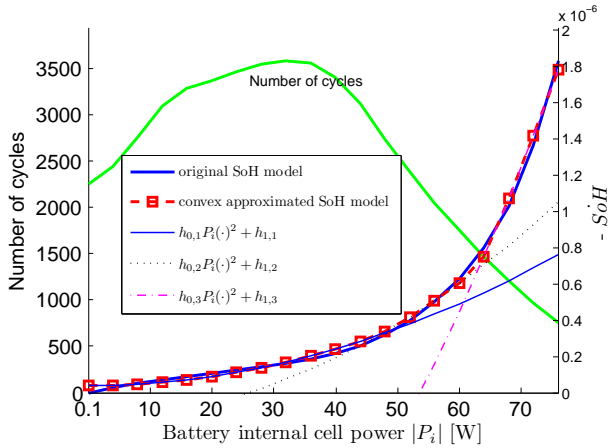


Fig. 5. Battery cell wear model. The number of cycles before end of life,  $N(|P_i|)$ , and the state of health derivative,  $\text{soh}(|P_i|)$ . The dashed red line show a piece-wise quadratic approximation of  $\text{soh}(|P_i|)$ . Note that 75 W corresponds to a c-rate of 9.2.

that calendar-life effects were not isolated when the model was built, i.e., the fact that  $N$  cycles take longer to process at low power than at high power, thereby exposing the battery to more calendar-life effects.

To ensure that battery is not worn out prematurely the degradation in SoH over the drive cycle is constrained

$$\text{soh}(t_0) - \text{soh}(t_f) \leq \Delta \text{soh} \quad (17)$$

#### 4. PROBLEM FORMULATION

The studied optimization problem is formulated to minimize a sum of operational cost for consumed fuel and electricity on the bus line and component cost for the EGU and the energy buffer. The costs are expressed in a single objective (18a) using the coefficients,  $w_f$  [currency/kWh], for the fuel, and  $w_b$ ,  $w_g$  in [currency], for the battery and EGU. The optimization problem is formulated as

$$\text{minimize} \int_{t_0}^{t_f} w_f P_f(\cdot) dt + w_b \mathbf{n}_b + w_g \mathbf{s} \quad (18a)$$

subject to (10b)-(17) and

$$\boldsymbol{\tau}(t) \geq \max \{ \tau_{\min}(\omega(t)), \tau_v(\cdot) \} \quad (18b)$$

$$\boldsymbol{\tau}(t)\omega(t) + B_{EM}(\cdot) \leq \mathbf{P}_b(t) + \mathbf{s}\mathbf{P}_{gb}(t) - P_a \quad (18c)$$

$$\mathbf{P}_{gb}(t) \in [0, P_{gbmax}e(t)] \quad (18d)$$

$$\mathbf{n}_b \geq 0, \quad (18e)$$

$$\mathbf{s} \in [0.5, 1.5], \quad (18f)$$

for all  $t \in [t_0, t_f]$  with optimization variables  $\mathbf{P}_b(t)$ ,  $\mathbf{P}_{gb}(t)$ ,  $\boldsymbol{\tau}(t)$ ,  $\text{soc}(t)$ ,  $\mathbf{n}_b$  and  $\mathbf{s}$ . With no effect on the optimal solution, the constraints (2) and (3) have been relaxed with inequalities in (18b) and (18c), respectively, and the braking torque has been taken out of the optimization problem, see Murgovski et al. (2012b) for details. The EGU price is assumed to follow an affine relation

$$c_{EGU} = c_0 + \mathbf{s}c_g$$

It is assumed that the payment of the EGU is divided in equal amounts over a period of  $y_g = 5$  years, with  $p = 5\%$

yearly interest rate. The equivalent EGU cost related to the driven bus line is obtained by multiplying the length of the bus line with the EGU's price per kilometer, given the average travel distance  $d$  in one year

$$w_g = c_g \left( 1 + p \frac{y_g + 1}{2} \right) \frac{\int_{t_0}^{t_f} v(t) dt}{y_g d},$$

with  $v(t)$  denoting the vehicle velocity demanded by the bus line. The the battery equivalent cost,  $w_b$  is calculated similary as the EGU cost

$$w_b = c_b \left( 1 + p \frac{y_b + 1}{2} \right) \frac{\int_{t_0}^{t_f} v(t) dt}{y_b d},$$

where the payment period for the battery and equivalently the expected life time,  $y_b$ , is a function of the number of battery replacements,  $n_r$ , during the EGU payment period  $y_g$ .

$$y_b = \frac{y_g}{n_r + 1}.$$

The allowed SoH degradation over the drive cycle is then

$$\Delta \text{soh} = \frac{\int_{t_0}^{t_f} v(t) dt}{y_b d}. \quad (19)$$

#### 5. CONVEX MODEL

This section presents the convexified version of the problem (18). The convex modeling approach of the battery from Section 5.2 is described in detail in Murgovski et al. (2012a) but the main steps are presented here for completeness. The modelling follows a disciplined methodology Boyd and Vandenberghe (2004) where the convexity of complex functions is verified using operations that preserve convexity of elementary convex functions, e.g. affine  $f(\mathbf{x}) = \mathbf{q}\mathbf{x} + r$ , quadratic  $f(\mathbf{x}) = \mathbf{p}\mathbf{x}^2 + \mathbf{q}\mathbf{x} + r$  with  $\mathbf{p} \geq 0$ , quadratic-over-linear  $f(\mathbf{x}, \mathbf{y}) = \mathbf{x}^2/\mathbf{y}$  with  $\mathbf{y} > 0$ , negative geometric mean  $f(\mathbf{x}, \mathbf{y}) = -\sqrt{\mathbf{x}\mathbf{y}}$  with  $\mathbf{x} \geq 0, \mathbf{y} \geq 0$ , etc.

##### 5.1 Convex EGU model

The EGU can be modeled as convex by introducing a variable change  $\mathbf{P}_g(t) = \mathbf{s}\mathbf{P}_{gb}(t)$  that eliminates the non-convex product of two variables. The change affects  $P_f(\cdot)$  making the cost function (18a) convex. The constraint (18d) is also affected, but its convexity is preserved, yielding

$$P_f(\cdot) = a_0 \frac{\mathbf{P}_g^2(t)}{\mathbf{s}} + (a_1 + 1)\mathbf{P}_g(t) + \mathbf{s}a_2 e(t)$$

$$\mathbf{P}_g(t) \in [0, \mathbf{s}P_{gbmax}e(t)].$$

##### 5.2 Convex battery model

The battery open circuit voltage, illustrated in Fig. 4, can be approximated with a linear function<sup>2</sup>

$$\mathbf{u}(\text{soc}(t)) = d_0 \text{soc}(t) + d_1$$

that gives good fit within the allowed SOC range.

The variable change proposed in Murgovski et al. (2012a) replaces the open cell voltage with

$$\mathbf{E}(t) = \frac{C\mathbf{u}^2(t)\mathbf{n}_b}{2} \Rightarrow \dot{\mathbf{E}}(t) = C\mathbf{n}_b\mathbf{u}(t)\dot{\mathbf{u}}(t)$$

<sup>2</sup> Approximating the open circuit voltage with an affine function in SoC is equivalent to modeling the battery as an ideal capacitor

where the used  $C = 2Q/\bar{U}$ .<sup>3</sup> The battery dynamics and constraints (11) can be then written as

$$\dot{\mathbf{E}}(t) \leq -\frac{d_0}{R_c Q} \left( \mathbf{E}(t) - \sqrt{\mathbf{E}^2(t) - 2R_c C \mathbf{P}_b(t) \mathbf{E}(t)} \right) \quad (20a)$$

$$\mathbf{E}(t) \in \frac{C}{2} [u^2(\text{soc}_{min}), u^2(\text{soc}_{max})] \mathbf{n}_b \quad (20b)$$

$$\mathbf{E}(t_f) = \mathbf{E}(t_0) \quad (20c)$$

The bounds on the cell current (10b) and the constraint (10c) are expressed as bounds on the pack power

$$\mathbf{P}_b(t) \geq \sqrt{\frac{2\mathbf{E}(t)\mathbf{n}_b}{C}} i_{min} - R_c i_{min}^2 \mathbf{n}_b \quad (21a)$$

$$\mathbf{P}_b(t) \leq \frac{\mathbf{E}(t)}{2R_c C} \quad (21b)$$

$$\mathbf{E}(t) - \sqrt{\mathbf{E}^2(t) - 2R_c C \mathbf{E}(t) \mathbf{P}_b(t)} \leq i_{max} R_c \sqrt{2C \mathbf{E}(t) \mathbf{n}_b} \quad (21c)$$

For a detailed derivation of the intermediate steps necessary to get to (20) and (21) as well as the proof of convexity, please refer to Murgovski et al. (2012a).

### 5.3 Convex battery wear model

The SoH model from Section 3.1 is piece-wise approximated using the three quadratic curves shown in Fig. 5 leading to the following SoH model

$$\dot{\text{soh}}(t) \leq h_{0,j} P_i(\cdot)^2 + h_{1,j}, \quad j = 1, 2, 3, \quad (22)$$

where  $h_{0,j}$ ,  $j = 1, 2, 3$  all are negative. The reasoning behind (22) is as follows: if the battery wear is influencing the optimal design, constraint (19) must be activated for the optimal solution. Moreover, at all times one of the constraints in (22) must be active, since otherwise the battery is "worn out" more than necessary which would be non-optimal if the wear is influencing the optimal design.

Since the model in Section 3.1 is formulated and parameterized with experiments at the nominal SoC and nominal voltage,  $\bar{U}$ , whereas the battery model in 5.2 considers the open circuit voltage as an affine function of SoC, the following approximation is proposed when predicting the battery wear,

$$\begin{aligned} \frac{\dot{\mathbf{E}}(t)}{\mathbf{n}_b} &= C \mathbf{u}(t) \dot{\mathbf{u}}(t) = C \mathbf{u}(t) d_0 \text{soc}(\cdot) = \\ \frac{2Q}{\bar{U}} \mathbf{u}(t) \frac{d_0 i(\cdot)}{Q} &= \frac{2d_0}{\bar{U}} \mathbf{u}(t) i(\cdot) \approx \frac{2d_0}{\bar{U}} \bar{U} i(\cdot) = \frac{2d_0}{\bar{U}} P_i(\cdot). \end{aligned}$$

Using the variable change  $\tilde{\text{soh}}(t) = \mathbf{n}_b \text{soh}(t)$  and the approximated internal battery power as above, (22) is rewritten as

$$\dot{\tilde{\text{soh}}}(t) - h_{0,j} \frac{\bar{U}^2 \dot{\mathbf{E}}(t)^2}{4d_0^2 \mathbf{n}_b} - \mathbf{n}_b h_{1,j} \leq 0, \quad j = 1, 2, 3, \quad (23)$$

The constraints (23) are convex since  $\mathbf{n}_b > 0$  and  $\frac{\dot{\mathbf{E}}(t)^2}{\mathbf{n}_b}$  can be recognized as the quadratic-over-linear elementary convex function. The allowed SoH degradation over the drive cycle is then

$$\tilde{\text{soh}}(t_0) - \tilde{\text{soh}}(t_f) \leq \Delta \text{soh} \mathbf{n}_b. \quad (24)$$

<sup>3</sup> Note that  $\mathbf{E}$  is a scaled version of battery energy.

Table 2. Parameter values.

Vehicle frontal area	$A_f = 7.54 \text{ m}^2$
Aerodynamic drag coefficient	$c_d = 0.7$
Rolling resistance coefficient	$c_r = 0.007$
Wheel radius	$r = 0.509 \text{ m}$
Final gear	$\gamma = 4.7$
Vehicle mass without buffer and EGU	$m_{vb} = 13.7 \text{ t}$
EM inertia	$I_{EM} = 2.3 \text{ kgm}^2$
Inertia of final gear and wheels	$I = 41.8 \text{ kgm}^2$
Sampling time	1 s
Battery cell specific energy	0.39 MJ/kg
Battery cell resistance, $R_c$	0.01 Ohm
<hr/>	
$P_a = 7 \text{ kW}$ , $w_f = 0.15 \text{ €/kWh}$ , $m_{EGUb} = 800 \text{ kg}$	
$c_0 = 6450 \text{ €}$ , $c_g = 6450 \text{ €}$	

## 6. EXAMPLE OF POWERTRAIN SIZING

This section gives an example of optimal powertrain sizing and control of a city bus. Using the proposed battery wear model the main question is to study the optimal battery replacement strategy for different price scenarios of the battery cells.

### 6.1 Problem setup

The bus is equipped with a 220 kW EM and a 150 kW baseline EGU as in Fig. 3. Data for the city bus and the used battery cells are given in Table 2. The example is done for the bus line in Fig. 2, with four scenarios for the battery cost: 500, 750, 1000, and 1250 €/kWh, investigating the optimal sizing and operational cost with four different strategies for the number of battery replacements over the time period,  $y_g = 5$  [years]:  $n_r \in \{1, 2, 3, 4\}$ . Moreover, a zero replacement strategy ( $n_r = 0$ ) was tried finding no feasible solution.

The convex problem is written in a time discrete form and a parser is used, CVX Grant and Boyd (2010), to translate the problem in a general form of linear matrix inequalities required by the solver. More details on the problem post-treatment can be found in Murgovski et al. (2012b).

### 6.2 Results

An overview of the results are given in Fig. 6, showing operating cost (eur/km), total battery energy capacity, maximum EGU power, used SoC window ( $\Delta \text{SoC}$ ), percentage of total brake energy regenerated, and maximum c-rate for the four replacement strategies and the four battery cell cost scenarios. The first thing to note is that difference in operating cost is very small between having two or three replacements. However, by looking carefully the figure shows that the best replacement strategy for all battery cell cost scenarios is to size and use the battery so that it needs two replacements over the period of five years. Although the operating cost is relatively similar between the different replacement strategies, the same thing cannot be said about the optimal battery size and the percentage of total brake energy regenerated which changes significantly between the different replacement strategies. The reason is that (17) is active in all the shown results, which simply means that the battery is sized and used to last according to the replacement strategy. Thus, the battery is

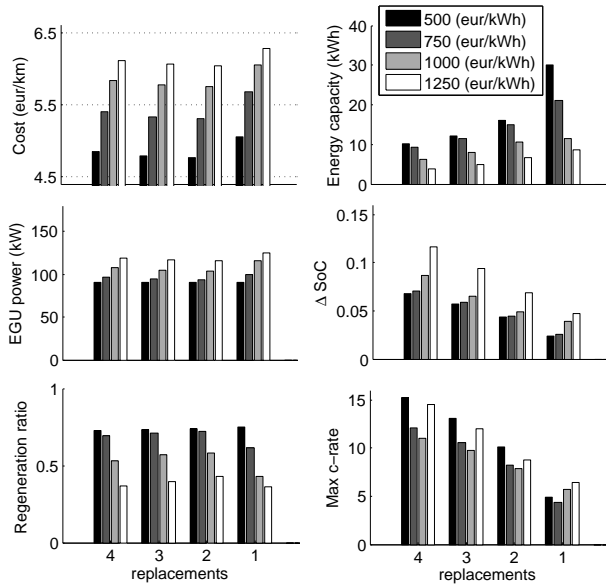


Fig. 6. Optimization study considering battery wear: The figure shows the optimal sizing and operational cost (cost of EGU, battery and fuel) with four different battery cell cost scenarios and with 1 to 4 battery replacements over the bus expected life time

almost three times bigger with one replacement compared to with four. This means that with one replacement, the used SoC window will be less than 5%. Moreover, the results show that both the percentage of total brake energy regenerated into the battery and the EGU size depend primarily on the battery cell cost and only slightly on the replacement strategy.

In Fig. 7 histograms of the norm of the internal battery cell power,  $|P_i|$ , are shown for the battery cell cost scenario of 1000 €/kWh. With fewer replacements the power distribution is compressed to lower power levels. The increasingly damaging power levels above 35 W are only used if the battery is to be replaced at least two times. With only one battery replacement, a significant part of the total battery wear is induced at power levels below 20 W where the calendar-life effects are predominant. These calendar-life effects explains why no feasible solution could be found for the zero replacement strategy, since at these low power levels simply doubling the battery size of the two replacement strategy will not result in twice as long battery life.

## 7. CONCLUSION AND DISCUSSION

The results clearly illustrate the importance of including the battery wear into the component sizing and optimal control problem. This expansion of the problem formulation with the inclusion of a battery wear model is practically feasible in the convex optimization approach since computational complexity is polynomial in the number of dynamic states.

The studied battery model relates battery wear to c-rate and is based on experimental data. However, for use in optimization studies it would be preferable to use a battery wear model that separate the calendar-life effects.

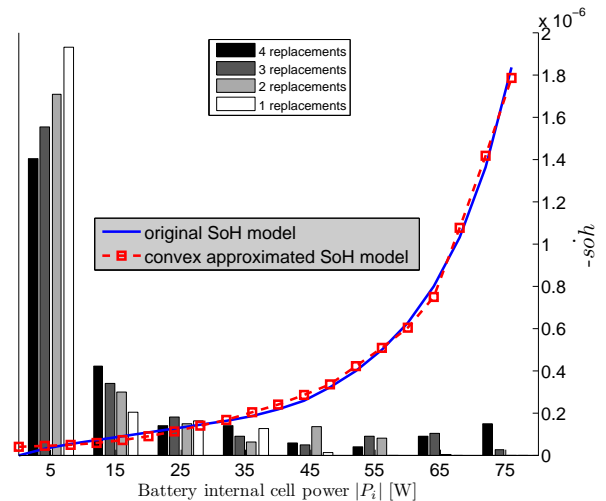


Fig. 7. Histogram of internal battery power: The figure shows the distribution of  $|P_i|$  for the different replacement strategies with the battery cost scenario of 1000 €/kWh.

## REFERENCES

- Boyd, S. and Vandenberghe, L. (2004). *Convex Optimization*. Cambridge University Press.
- Ebbesen, S., Elbert, P., and Guzzella, L. (2012). Battery state-of-health perceptive energy management for hybrid electric vehicles. *IEEE Transactions on Vehicular Technology*.
- Grant, M. and Boyd, S. (2010). CVX: Matlab software for disciplined convex programming, version 1.21. <http://cvxr.com/cvx>.
- I. Bloom, B., Cole, J.S., Jones, S., Polzin, E., Battaglia, V., Henriksen, G., Motloch, C., Richardson, R., Unkelhaeuser, T., Ingersoll, D., and Case, H. (2001). An accelerated calendar and cycle life study of li-ion cells. *Journal of Power Sources*, 101(2), 238247.
- Murgovski, N., Johannesson, L., and Sjöberg, J. (2012a). Convex modeling of energy buffers in power control applications. In *IFAC Workshop on Engine and Powertrain Control, Simulation and Modeling (ECOSM)*. Rueil-Malmaison, Paris, France.
- Murgovski, N., Johannesson, L., Sjöberg, J., and Egardt, B. (2012b). Component sizing of a plug-in hybrid electric powertrain via convex optimization. *Journal of Mechatronics*, 22(1), 106–120.
- Sundström, O., Guzzella, L., and Soltic, P. (2010). Torque-assist hybrid electric powertrain sizing: From optimal control towards a sizing law. *IEEE Transactions on Control Systems Technology*, 18(4), 837–849.
- Wang, J., Liu, P., Hicks-Garner, J., Sherman, E., Soukiazian, S., Verbrugge, M., Tatara, H., Musser, J., and Finamore, P. (2011). Cycle-life model for graphite-lifepo4 cells, journal of power sources. *Journal of Power Sources*, 196 (8), 39423948.
- Zoelch, U. and Schroeder, D. (1998). Dynamic optimization method for design and rating of the components of a hybrid vehicle. *International Journal of Vehicle Design*, 19(1), 1–13.